The American Journal of Pathology, Vol. 175, No. 1, July 2009

DOI: 10.2353/ajpath.2009.081002

Cell Injury, Repair, Aging and Apoptosis

A Transgenic Mouse Model of Inducible Macrophage Depletion

Effects of Diphtheria Toxin-Driven Lysozyme M-Specific Cell Lineage Ablation on Wound Inflammatory, Angiogenic, and Contractive Processes

Itamar Goren,* Nadine Allmann,* Nir Yogev,† Christoph Schürmann,* Andreas Linke,* Martin Holdener,* Ari Waisman,† Josef Pfeilschifter,* and Stefan Frank*

From the Pharmazentrum Frankfurt/*ZAFES,* Klinikum der Johann Wolfgang Goethe-Universität, Frankfurt am Main, Germany; and the I. Medizinische Klinik und Poliklinik,† Johannes Gutenberg Universität Mainz, Mainz, Germany*

Whether the wound macrophage is a key regulatory inflammatory cell type in skin repair has been a matter of debate. A transgenic mouse model mediating inducible macrophage depletion during skin repair has not been used to date to address this question. Here, we specifically rendered the monocyte/macrophage leukocyte lineage sensitive to diphtheria toxin by expressing the *lysozyme M* promoter-driven, Cre-mediated excision of a transcriptional STOP cassette from the simian DT receptor gene in mice (*lysM*-Cre/DTR). Application of diphtheria toxin to *lysM*-Cre/DTR mice led to a rapid reduction in both skin tissue and wound macrophage numbers at sites of injury. Macrophage-depleted mice revealed a severely impaired wound morphology and delayed healing. In the absence of macrophages, wounds were re-populated by large numbers of neutrophils. Accordingly, macrophage-reduced wound tissues exhibited the increased and prolonged persistence of macrophage inflammatory protein-2, macrophage chemoattractant protein-1, interleukin-1β, and cyclooxygenase-2, paralleled by unaltered levels of bioactive transforming growth factor-β1. Altered expression patterns of vascular endothelial growth factor on macrophage reduction were associated with a disturbed neo-vascularization at the wound site. Impaired wounds revealed a loss of myofibroblast differentiation and wound contraction. Our data in the use of lysM-Cre/DTR mice emphasize the pivotal function of wound macrophages in the integration of inflammation and cellular movements at the wound site to enable efficient skin repair. ***(Am J Pathol 2009, 175:132–147; DOI: 10.2353/ajpath.2009.081002)***

A comprehensive set of different strategies has been used during the past three decades to explore the function and impact of inflammatory cell lineages on tissue regeneration processes in skin wounds. The field was opened by two pioneer studies by Simpson and Ross[1] and Leibovich and Ross.[2] Both classic experiments assessed neutrophil and macrophage functions: neutrophil depletion did not impact on healing, but depletion of macrophages resulted in an impaired clearance of wound tissue and a severe disturbance of the healing process. These early studies provided the insight that the presence of macrophages at the wound site might appear central to skin repair. This notion was supported by more recent studies. Inactivation of the chemokine macrophage inflammatory protein (MIP)-1α,[3] as well as genetic knock-out of the CXC chemokine receptor 2[4] markedly reduced wound macrophage numbers and delayed

Supported by the Deutsche Forschungsgemeinschaft (SFBs 553 and 815, grant FR 1540/1-2, GK 1172, Excellence Cluster Cardio-Pulmonary System) and Else-Kroener-Fresenius-Stiftung.

I.G. and N.A. contributed equally to this work.

Accepted for publication March 19, 2009.

Supplemental material for this article can be found on *http://ajp.amjpathol.org.*

Address reprint requests to Dr. Stefan Frank, *Pharmazentrum frankfurt*, Institut für Allgemeine Pharmakologie und Toxikologie, Klinikum der JW Goethe-Universität Frankfurt/M., Theodor-Stern-Kai 7, D-60590 Frankfurt/M., Germany. E-mail: S.Frank@em.uni-frankfurt.de.

wound healing by impairing angiogenesis and collagen deposition. Proper activation of wound macrophages appeared to be also of importance: apoptotic neutrophils induced secretion of transforming growth factor (TGF)-β1 from macrophages, which is necessary to subsequently drive myofibroblast differentiation and wound contraction.[5] Moreover, macrophage-chemoattractant protein (MCP)-1 deficient mice exhibited unaltered numbers of wound macrophages on wounding, but showed a delayed re-epithelialization, angiogenesis, and collagen synthesis.[6] At present, the wound macrophage is established as a key player in undisturbed cutaneous wound healing, mainly in its function as a rich source of mediators at the wound site.[7–10]

A set of studies recently came out that might carry the potential to question the fundamental role of the wound macrophages in skin repair. One of those studies demonstrated the 'paradoxical' finding of an improved wound healing on interference with TGF-β1 signaling using a SMAD-3 deficiency. Wounds of SMAD-3 knock-out mice were characterized by a reduced local infiltration of monocytes associated with an accelerated re-epithelialization.[11] In addition, disruption of tumor necrosis factor-α signaling led to a significant reduction in wound macrophages and an accelerated repair.[12] More important, studies from embryos and the PU.1 transcription factor knock-out mouse support the notion of an ambivalent role of macrophage function in skin repair. Wounds in embryos healed without excessive inflammation and scarring as long as the monocyte lineage has not developed.[13] Loss of PU.1 results in the loss of macrophages and functional neutrophils in mice. However, wounds from PU.1 null mice showed a scar-free, 'embryo-like' healing without inflammation.[14] These important studies might suggest that the inflammatory response on wounding might only serve the function to prevent infection for the price of an impaired, fibrotic repair and formation of a scar.

However, having a second glance on the above mentioned classic and more recent studies on macrophage function in wound healing, some difficulties in the interpretation of findings become obvious: the anti-inflammatory corticosterone has been used to fully deplete macrophages from wounds in the early studies,[2] wounds had to be kept sterile to enable normal healing,[1,14] or transgenic knock-out animals must always be considered to potentially develop a compensatory adaptation. To circumvent these problems, we have used a transgenic mouse (*lysM*-Cre/DTR) containing diphtheria-toxin (DTox)-sensitive macrophages to assess macrophage functions in wound healing. *LysM*-Cre/DTR mice express a normal phenotype in the absence of the toxin.[15] Application of DTox allowed a simple, inducible, and rapid depletion of macrophages from wound tissue, thus circumventing problems that might arise from conventional knock-out strategies. In this study, we show the functionality of the *lysM*-Cre/DTR mouse model to investigate macrophage functions in skin repair. Our data strengthen the evidence that macrophages indeed represent an essential prerequisite for overall tissue regeneration.

Materials and Methods

Animals

Using the *loxP* system, we established a conditional myeloid cell linage-specific expression of the DTox receptor (DTR) by crossing C57Bl/6-*ROSA26*STOP*DTR mice[15] with C57Bl/6-*LysM*-Cre mice.[16] Mice were kept in barrier and specific pathogen-free animal facilities according to the German Tierschutzgesetz. DNA for genotyping was prepared from tail biopsies. Presence of different alleles was assessed by PCR using the following primer pairs: for wild-type (wt)*ROSA26S* (600 bp amplicon) 5′-AAAGTCGCTCTGAGTTGTTAT-3′ and 5′-GGAGCGGGAGAAATGGATATG-3′, for *ROSA26S*/DTR (242 bp amplicon) 5′-AAAGTCGCTCTGAGTTGTTAT-3′ and 5′-CATCAAGGAAACCCTGGACTACTG-3′, for wild-type (wt) *lysM* (350 bp amplicon) 5′-CTTGGGCTGCCAGAATTTCTC-3′ and 5′-TTACAGTCGGCCAGGCTGAC-3′, and *lysM*-Cre (700 bp amplicon) 5′-CTTGGGCTG CCAGAATTTCTC-3′ and 5′-CCCAGAAATGCCAGATTACG-3′.

Treatment of Mice

At the age of 12 weeks, mice were caged individually, monitored for body weight and wounded as described below. For cell-type specific cell ablation, age- and sex-matched *lysM*-Cre/DTR mice were injected intraperitoneally for three consecutive days with 100 ng of recombinant DTox (Calbiochem, Darmstadt, Germany) before wounding. Injection of PBS was used as a control. After wounding, mice were injected with DTox or PBS every second day. Topical treatment of *lysM*-Cre/DTR mice was performed by application of recombinant DTox (25 ng in 20 μl PBS/5% dimethylsulfoxide) directly onto wound sites at days 0, 2, and 4 after wounding. Mice were injected intraperitoneally with a single injection of 0.5 ml of sterile thioglycollate (Sigma, Taufkirchen, Germany) solution (6% w/v in H_2O) to induce peritonitis. At 60 hours after injection, mice were sacrificed to isolate cells from the peritoneal cavity.

Wounding of Mice

Wounding of mice was performed as described previously.[17,18] Briefly, mice were anesthetized with a single intraperitoneal injection of ketamine (80 mg/kg body weight)/xylazine (10 mg/kg body weight). The hair on the back of each mouse was cut, and the back was subsequently wiped with 70% ethanol. Six full-thickness wounds (5 mm in diameter, 3 to 4 mm apart) were made on the back of each mouse by excising the skin and the underlying *panniculus carnosus*. The wounds were allowed to form a scab. Skin biopsy specimens were obtained from the animals 1, 3, 5, 7, and 13 days after injury. At each time point, an area that included the scab, the complete epithelial and dermal compartments of the wound margins, the granulation tissue, and parts of the adjacent muscle and subcutaneous fat tissue was ex-

cised from each individual wound. As a control, a similar amount of skin was taken from the backs of nonwounded mice. Wounds ($n = 15$) isolated from animals ($n = 5$) were used for RNA analysis. For immunoblot analysis, wounds ($n = 10$) from individual mice ($n = 5$) were used. All animal experiments were performed according to the guidelines and approval of the local Ethics Animal Review Board.

RNA Isolation and RNase Protection Analysis

RNA isolation and RNase protection assays were performed as described previously.[18,19] If not indicated otherwise, every experimental time point depicts 15 wounds ($n = 15$) isolated from five individual mice ($n = 5$) for all RNase protection assays analyzing wound tissues samples. All samples were quantified using PhosphoImager PSL counts per 15 μg of total wound RNA. Glyceraldehyde phosphate dehydrogenase (GAPDH) hybridization is shown as a loading control and 1000 cpm of the hybridization probe were used as a size marker. Hybridization against tRNA was used to show the specificity of the probe. The murine cDNA probes were cloned using reverse transcriptase-polymerase chain reaction. The probes corresponded to nucleotides (nt) 181 to 451 (for *MIP-2*, GenBank accession number NM009140), nt 63 to 323 (for *MCP-1*, NM011333), nt 816 to 1481 (for *lipocalin*, X81627), nt 425 (exon 1) to 170 (exon 2) (for *lysozyme M*, M21047), nt 481 to 739 (for *interleukin [IL]-1β*, NM008361), nt 796 to 1063 (for *Cox-2*, M64291), nt 2561 to 2783 (for epidermal growth factor[EGF]-like module-containing, mucin-like, hormone receptor-like sequence *[Emr]−1*, X93328), nt 139 to 585 (for vascular endothelial growth factor *[VEGF]*, S38083), nt 912 to 1183 (for α-smooth muscle actin *[α-SMA]*, BC064800.1), nt 1335 to 1594 (for extra type III domain A *[ED-A] fibronectin*, AF095690), nt 1274 to 1546 (for *TGF-β1*, NM-011577), or nt 163 to 317 (for murine *GAPDH*, NM002046) of the published sequences.

Quantitative Real-Time PCR

Quantitative real-time PCR (qRT-PCR) was performed to assess the expression of genes of interest in wound tissue at day 7 post-wounding. Changes in fluorescence are caused by the *Taq* polymerase degrading the probe that contains a fluorescent dye (6-carboxyfluorescein for the genes of interest, VIC for *GAPDH*) and a quencher (6-carboxytetramethylrhodamine). Pre-designed qRT-PCR assays were purchased at Applied Biosystems (Darmstadt, Germany): Mm00436450-m1 (for *MIP-2*), Mm00441242-m1 (for *MCP-1*), Mm01324470-m1 (for *lipocalin*), Mm00802529-m1 (for *Emr-1*), Mm00478374-m1 (for *Cox-2*), or Mm00437404-m1 (for *VEGF*). The possibility of amplification of contaminating genomic DNA was eliminated by the fact that amplicons crossed an exon/intron boundary. For *GAPDH*, pre-developed assay reagents were used (4352339E) (Applied Biosystems, Darmstadt, Germany). 1.0 μg of total RNA from day 7 wound tissue was transcribed using random hexameric primers and Superscript II RT (Invitrogen, Karlsruhe, Germany) according to the manufacturer's instructions. qRT-PCR was performed on 7500 Fast real-time PCR system (Applied Biosystems) as follows: one initial step at 95°C for 20 seconds was followed by 40 cycles at 95°C for 3 seconds and 60°C for 30 seconds. Detection of the dequenched probe, calculation of threshold cycles (*Ct* values), and further analysis of these data were performed by the Sequence Detector software. All results for gene expression were normalized to that of *GAPDH*.

Reverse Transcription-PCR

Reverse transcription (RT) PCR was performed to assess the expression of lysozyme M, Cre recombinase and GAPDH in isolated murine immune cell fractions. 1.0 μg of total RNA from the respectice immune cell fraction was transcribed using random hexameric primers and Superscript II RT (Invitrogen, Karlsruhe, Germany) according to the manufacturer's instructions. 5′-ATTGCAGTGCTCTGCTGC-3′ and 5′-GTGAGAAAGAGACCGAATG-3′ (for *lysM*), 5′-GTGTCCAATTTACTGACCG-3′ and 5′-GTTTTTACTGCCAGACCGC-3′ (for *Cre*) or 5′-CTGGCATTGCTCTCAATGAC-3′ and 5′-TCTTACTCCTTGGAGGCC-3′ (for *GAPDH*) primers were used to amplify the murine sequences. PCR was performed on a T3000-Thermocycler (Biometra, Göttingen, Germany).

Preparation of Protein Lysates and Western Blot Analysis

Skin and wound tissue biopsies were homogenized in lysis buffer (1% Triton X-100, 20 mmol/L Tris/HCl pH 8.0, 137 mmol/L NaCl, 10% glycerol, 1 mmol/L dithiothreitol, 10 mmol/L NaF, 2 mmol/L Na_3VaO_4, 5 mmol/L EDTA, 1 mmol/L phenylmethylsulfonylfluoride, 5 ng/ml aprotinin, 5 ng/ml leupeptin). Wound lysates for cell culture experiments were homogenized in PBS. Extracts were cleared by centrifugation. Protein concentrations were determined using the BCA Protein Assay Kit (Pierce Inc., Rockford, IL). Fifty micrograms of total protein from skin lysates were separated using SDS gel electrophoresis. After transfer to a nitrocellulose membrane, specific proteins were detected using antisera raised against Ly-6G (GR-1) (BD Biosciences, Heidelberg, Germany), Cox-2 (Cayman, Ann Arbor, MI), α-SMA (Dako, Glostrup, Denmark), and β-actin (Sigma). A secondary antibody coupled to horseradish peroxidase and the enhanced chemiluminescence detection system was used to visualize the proteins. Phenylmethylsulfonyl fluoride, dithiothreitol, aprotinin, NaF, and Na_3VaO_4 were from Sigma. Leupeptin and ocadaic acid were from BioTrend (Köln, Germany). The enhanced chemiluminescence detection system was obtained from Amersham (Freiburg, Germany).

Enzyme-Linked Immunosorbent Assay

Quantification of murine MIP-2, MCP-1, IL-1β, or $VEGF_{165}$ protein was performed using the respective murine quantikine enzyme-linked immunosorbent assay (ELISA) kits

(R&D Systems, Wiesbaden, Germany) according to the instructions of the manufacturer. Human IL-8 ELISA kit was obtained from BD Biosciences.

Immunohistochemistry

Wounding of mice was performed as described above. Animals were sacrificed following the 3-day DTox pretreatment or at day 5 and 7 after injury. Biopsies from non-wounded skin and skin wounds were isolated from the back, fixed in formalin or in zinc fixative solution (0.05% $CaAc \cdot 2H_2O$, 0.5 $ZnAc \cdot 2H_2O$, 0.5% $ZnCl_2$ in 0.1 M/L Tris-Cl, pH 7.4) and subsequently embedded in paraffin. Four-micrometer sections were counterstained with H&E to document overall wound morphology. Sections were subsequently incubated over night at 4°C with antisera raised against murine MIP-2 (R&D), Cox-2 (Biomol, Hamburg, Germany), Ly-6G (Gr-1), F4/80 (AbD Serotec, Düsseldorf, Germany), processed active caspase-3 (DCS Inc., Hamburg, Germany), VEGF (Santa Cruz, Heidelberg, Germany), CD31 (Chemicon, Eschborn, Germany), or α-SMA (Sigma). Primary antibodies were detected using a biotinylated secondary antibody. The slides were subsequently stained with the avidin-biotin-peroxidase complex system (Santa Cruz) using 3,3-diaminobenzidine tetrahydrochloride or Fast Red Substrate-Chromogen System (Dako, Hamburg, Germany) as a chromogenic substrates. Finally, sections were counterstained with hematoxylin and mounted.

Cell Culture

Isolated femur and tibia from mice were flushed out using BMDC medium (Gibco, Invitrogen) to obtain the bone marrow content for cell culture. Cells were collected by centrifugation (250 $\times$ *g*), and 2 $\times$ 10^6 cells per dish (10 cm) were plated. Cells were cultured in the presence of a granulocyte-monocyte colony-stimulating factor containing hybridoma cell culture supernatant (5% v/v) to obtain non-adherent and adherent cell fractions. Isolated cell fractions were analyzed by flow cytometry (see below).

Primary keratinocytes were isolated from skin of newborn C57Bl/6J mice (1 to 3 days) by overnight incubation using dispase (2.4 U/ml, 4°C). After dispase (Roche Biochemicals, Mannheim, Germany) digestion, the epidermis could be isolated and was subsequently treated with trypsin (0.04%)/EDTA (0.03%) for additional 7 minutes to disaggregate cells. After filtration (70 μm; Falcon, Becton Dickinson Labware), keratinocytes were collected by centrifugation (210 $\times$ *g*, 2 minutes) and plated into collagen IV-coated dishes. Confluent murine keratinocytes were treated with a combination of IL-1β (40 ng/ml), tumor necrosis factor-α (25 ng/ml), and interferon-γ (20 ng/ml) in the presence or absence of TGF-β1 (5 ng/ml).

The human keratinocyte cell line HaCaT[20] was cultured in Dulbecco's Modified Eagle Medium containing 10% (v/v) fetal calf serum. Quiescent confluent keratinocytes were subsequently stimulated using freshly prepared 5-day wound tissue homogenates (f.c: 100 μg of total protein per ml) isolated from *lysM*-Cre/DTR in the presence or absence of a neutralizing anti-TGF-β1-3 antibody (clone 1D11) (100 μg/ml) or IL-1 receptor antagonist (IL-1ra) (500 ng/ml) for 24 hours. Dulbecco's Modified Eagle Medium and fetal calf serum were from Gibco (Invitrogen), cytokines were purchased from Roche, anti-TGF-β1-3 and IL-1ra were from R&D systems.

Isolation of Neutrophils

Polymorphonuclear neutrophils were freshly isolated from mouse blood using a standard protocol. Briefly, 400 μl ACD (3% w/v citric acid, 6% w/v sodium citrate, 4% dextrose) were added to 2 ml of mouse blood; 1.2 ml of 6% dextran in 0.9% NaCl was added subsequently and blood was incubated for 1 hour at room temperature. The supernatant was recovered from the settled blood and centrifuged (280 $\times$ *g*). The cellular pellet was suspended in 1.2 ml ice-cold H_2O, and 400 μl of 0.6 M/L KCl was added. Mixture was centrifuged to remove red blood cells. Red blood cell-free cells were again centrifuged through a Ficoll-Histopaque (Sigma) gradient to finally isolate a pure neutrophil cellular pellet. The isolated cell fraction was analyzed for the expression of Ly6G (GR-1) (BD Biosciences).

Flow Cytometry

Two hundred microliters of blood from *lysM*-Cre/DTR mice were collected in 5 ml RPMI medium. Blood cells were harvested by centrifugation and treated with 5 ml lysis buffer (0.83% NH_4CL) for 5 minutes to lyse erythrocytes. The remaining leukocytes were washed in 5 ml of fresh RPMI medium. Leukocytes were collected and resuspended in 3 ml staining buffer (PBS supplemented with 1% v/v fetal calf serum and 0.1% Na_3N). The resuspended pellet was subsequently incubated in 50 μl of phycoerythin-conjugated rat anti-mouse F4/80 (AbD Serotec) in staining buffer at 4°C for 30 minutes, followed by two additional washing steps in 3 ml of staining buffer. Cells were fixed (fluorescence-activated cell sorting [FACS] buffer containing 1% paraformaldehyde) and analyzed for surface F4/80 expression using a FACSCalibur flow cytometer (BD Biosciences). Monocyte and macrophage cell fractions obtained from cultured bone marrow cells or by peritoneal lavage were analyzed using Cy7-conjugated CD11b (mac1), phycoerythin-conjugated F4/80, and fluorescein isothiocyanate-labeled Ly6C (BD Biosciences).

In Vitro *Assay to Determine TGF-β Bioactivity from Wound Lysates*

TGF-β bioactivity was determined using an *in vitro* assay based on mink lung epithelial cells containing a truncated TGF-β sensitive *plasminogen activator inhibitor-1* promoter fused to the firefly *luciferase* reporter gene.[21] Wounds were homogenized in PBS and mink cells were stimulated with wound lysates (400 μg lysate per ml) in the presence or absence of a TGF-β neutralizing antibody

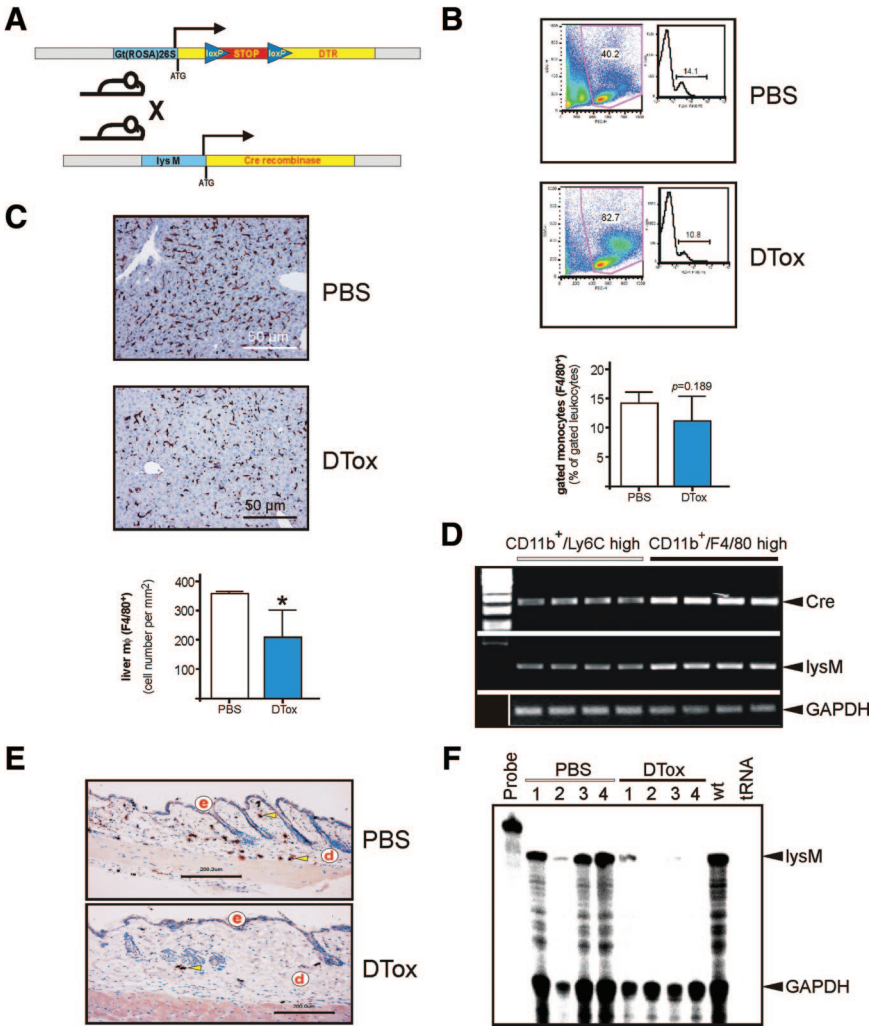

Figure 1. Inducible macrophage depletion in *lysM*-Cre/DTR mice. **A:** Scheme of the inducible DTR mouse strain. The STOP cassette, which prevents expression of the functional DTR, is removed by crossing the DTR mouse strain to a *lysM*-Cre myeloid cell lineage-specific Cre-expressing mouse strain. Consecutive expression of the DTR renders the respective tissue sensitive to cell death induced by injection of DT. **B:** Circulating F4/80-positive monocytes in *lysM*-Cre/DTR mice. Mice had been injected with PBS or DTox (for three consecutive days) as indicated. Fresh blood was analyzed for F4/80-positive monocytes by FACS. One representative animal for each treatment is shown, a statistical analysis is given below. $P = 0.189$ (unpaired Student's *t*-test) versus PBS-treated mice. Bars indicate the mean ± SD from five individual animals ($n = 5$). **C:** Immunohistological quantification of F4/80-positive liver tissue macrophages (Kupffer cells). Mice had been injected with PBS or DTox (for three consecutive days) as indicated. Representative sections from PBS- and DTox-treated mice are shown. Absolute numbers of F4/80-positive macrophages from analyzed liver sections are given in the **lower panel**. $^*P < 0.05$ (unpaired Student's *t*-test) versus PBS-treated mice. Bars indicate the mean ± SD from five individual animals ($n = 5$). **D:** RT-PCR analyses showing Cre and lysM mRNA expression in monocytes ($CD11b^+$/Ly6C high) and macrophages ($CD11b^+$/F4/80 high) as indicated. Four independent preparations from bone marrow are shown for each cell fraction. An amplification of GAPDH is shown for equal loading. **E:** Paraffin sections from non-wounded skin isolated from PBS- and DTox-injected mice as indicated were incubated with an antibody directed against macrophage-specific F4/80 protein. Sections were stained with the avidin-biotin-peroxidase complex system. Nuclei were counterstained with hematoxylin. Immunopositive signals were indicated by yellow **arrows**. Scale bars are given in the photographs. d, dermis; e, epidermis. **F:** Lysozyme M mRNA expression in non-wounded skin tissue isolated from PBS- and DTox-injected mice as indicated. Mice had been injected with PBS or DTox (for three consecutive days) before analysis. #1–4 represent individual animals. For the RNase protection assay, every experimental time point depicts three wounds ($n = 3$) isolated from a single individual mouse. GAPDH hybridization is shown as a loading control; 1000 cpm of the hybridization probe were used as a size marker. Hybridization against tRNA was used to show the specificity of the probe.

(clone 1D11) (100 µg/ml) (R&D systems). After 20 hours, cells were washed and lysed in 100 µl lysis buffer (Promega, Mannheim, Germany) to determine the induced luciferase activity using a standard protocol.

Statistical Analysis

Data are shown as means ± SD. Data analysis was performed using the unpaired Student's *t*-test with raw data.

Results

Generation of a Transgenic Mouse Sensitive to a DTox-Mediated Myeloid Cell Lineage Ablation

Transgenic expression of the DTR, which is identical to the simian/human heparin-binding epidermal growth factor-like growth factor precursor,[22] represents a molecule to render naturally DTox-resistant mouse cells[23] susceptible to DTox.[24] Here we crossed the *ROSA26*STOP*DTR transgenic mouse strain,[15] harboring the simian DTR (simian HB-EGF), containing a *loxP*-flanked transcriptional STOP cassette, under control of the *ROSA26* locus,[25] into *lysM*-Cre mice. Cre-mediated excision of the STOP cassette in *lysM*-Cre/DTR double-transgenic mice subsequently allows the expression of a functional DTR in myeloid cells in the animals[16,26] (Figure 1A). Genotyping by PCR revealed a decisive amplicon pattern to allow selection of *lysM*-Cre/DTR double-transgenic mice (see supplemental Figure S1 available at *http://ajp.amjpathol.org*). Here it is noteworthy that we selected those *lysM*-Cre/DTR transgenic mice for subsequent studies, which were characterized by the insertion of only one allele of the *lysM*-Cre construct to allow functional expression of endogenous lysozyme M in the animals from the second allele.

To assess the functionality of the inducible DTR-driven cell ablation sytem *in vivo*, we analyzed the response of

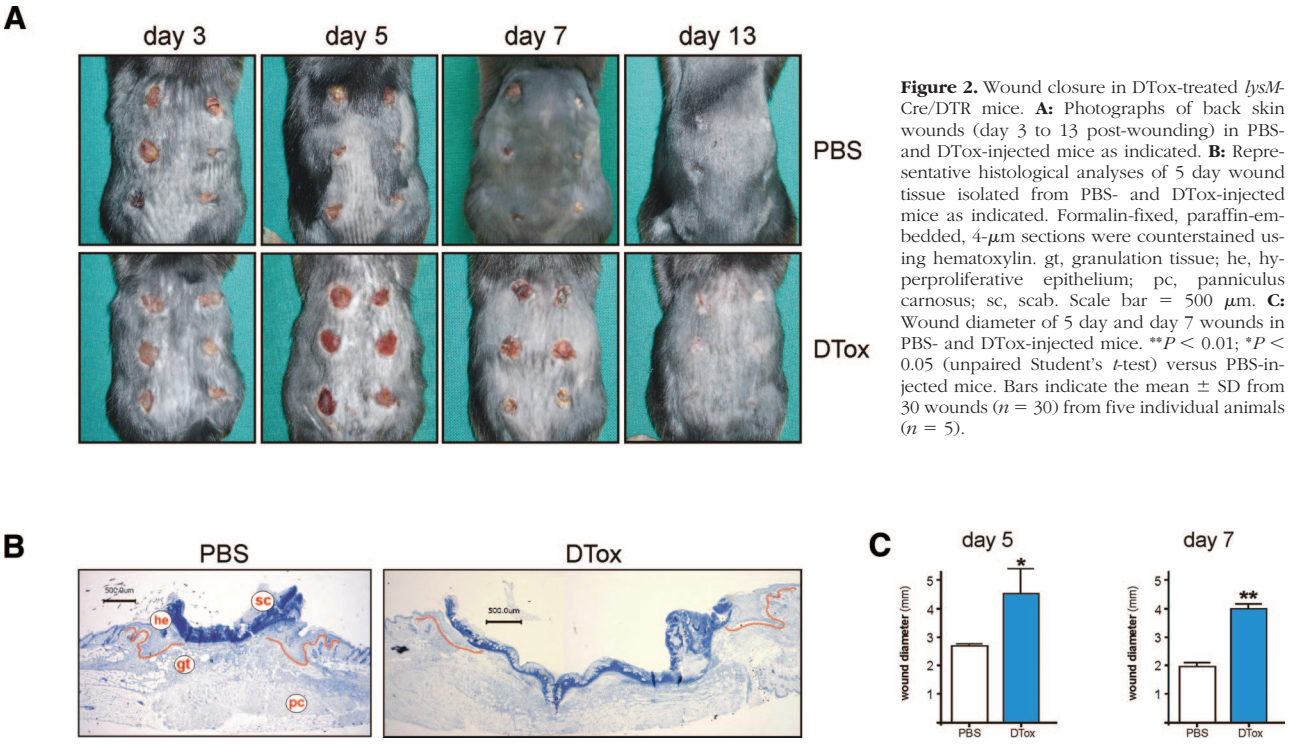

Figure 2. Wound closure in DTox-treated *lysM*-Cre/DTR mice. **A:** Photographs of back skin wounds (day 3 to 13 post-wounding) in PBS- and DTox-injected mice as indicated. **B:** Representative histological analyses of 5 day wound tissue isolated from PBS- and DTox-injected mice as indicated. Formalin-fixed, paraffin-embedded, 4-μm sections were counterstained using hematoxylin. gt, granulation tissue; he, hyperproliferative epithelium; pc, panniculus carnosus; sc, scab. Scale bar = 500 μm. **C:** Wound diameter of 5 day and day 7 wounds in PBS- and DTox-injected mice. $^{**}P < 0.01$; $^{*}P < 0.05$ (unpaired Student's *t*-test) versus PBS-injected mice. Bars indicate the mean ± SD from 30 wounds ($n = 30$) from five individual animals ($n = 5$).

the monocyte/macrophage lineage on DTox injection into transgenic *lysM*-Cre/DTR mice. As shown in Figure 1B, we could not observe a significant reduction in circulating monocyte numbers on DTox administration, which had been injected for three consecutive days before analysis. A reduced *lysozyme* M promoter activity in monocytes might, at least partially, contribute to ineffective levels of Cre recombinase and thus reduced expression of the DTR on the cells surface. As shown in Figure 1D, bone-marrow-derived, *in vitro*-differentiated macrophages (CD11b^{+}/F4/80 high) from *lysM*-Cre/DTR mice exhibited an increase in Cre mRNA when compared with monocytes (CD11b^{+}/Lys6C high). By contrast, staining of liver sections from the same individual mice for F4/80, which represents a monocyte/macrophage-specific protein,[27] exhibited a significant reduction in F4/80-positive tissue macrophages (Kupffer cells) on DTox-treatment (Figure 1C). Analysis of our target tissue of interest, the skin, showed that resident skin tissue macrophages could be efficiently depleted by a 3-day DTox administration (Figure 1E). In addition, we could confirm the nearly complete absence of tissue macrophages in non-wounded skin (Figure 1F), as assessed by RNase protection analysis of lysM mRNA, which has been used as reliable marker to determine the presence of macrophages in skin and wound tissue.[28,29]

DTox Administration into Mice Provokes Severely Disturbed Wounds by Ablation of Macrophages but not Neutrophils

As a next step, we wounded *lysM*-Cre/DTR mice in the presence or absence of systemic DTox. It turned out that application of the toxin markedly interfered with the normal healing process of cutaneous full-thickness wounds (Figure 2A). Histological analysis revealed that DTox-mediated impairment of wound tissue was primarily characterized by failure of the injured tissue to contract and thus reduce wound diameter during acute as well as late repair (Figure 2, B and C).

As a next step, we had to connect the observed impairment of wound healing as a function of the expected particular DTox-mediated ablation of macrophages in our transgenic *lysM*-Cre/DTR model. As we had targeted the functional DTR under control of the *lysM* promoter, we had to keep in mind that also granulocytes/neutrophils as members of the myeloid cell lineage might be impacted by *lysM*-Cre mediated activation of the DTR[16,26] and contribute to the observed tissue defects. To this end, we first determined the expression of Emr-1 mRNA, which represents the transcript of the macrophage-specific marker F4/80.[27,30] We observed a marked reduction of Emr-1 transcripts during acute repair (Figure 3A). Topical application of DTox (25 ng per wound in 20 μl PBS) was not effective to deplete macrophages from wounded sites (see supplemental Figure S2 available at *http://ajp.amjpathol.org*). LysM mRNA as an additional marker of macrophages[28,29] was strongly reduced in 1-day wounds (Figure 3B), although also neutrophils express a potentially functional *lysM* promoter.[16,26] Nevertheless, it is important to note that analysis of lysM mRNA expression revealed a robust presence in both PBS- and DTox-treated mice starting at day 3 post-wounding (Figure 3, C–F). This was exactly that time of repair, when we first observed large numbers of neutrophils at the wound site as assessed by lipocalin mRNA expression (Figure 4A). Impaired wounds (day 7) were characterized by reduced

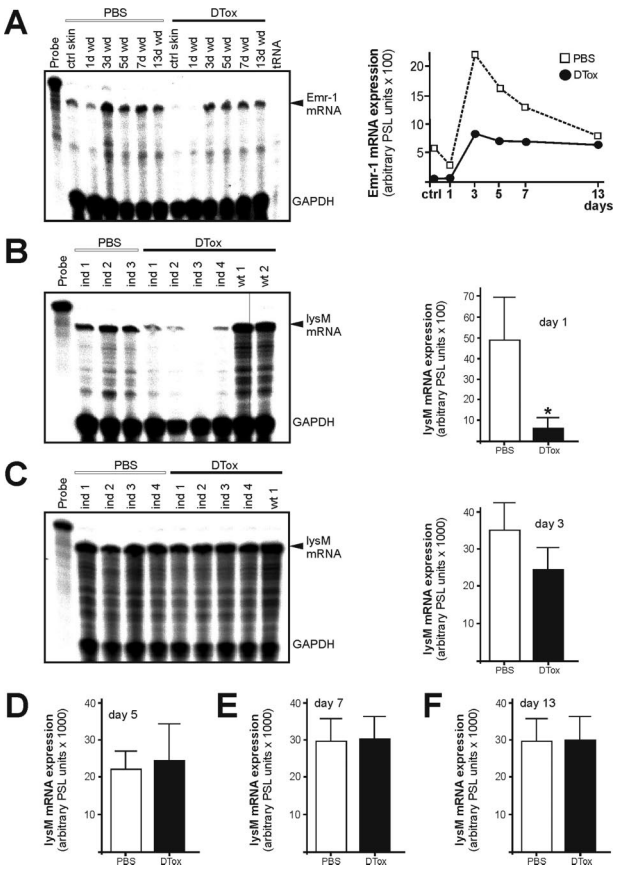

Figure 3. Analysis of wound macrophages in DTox-injected *lysM*-Cre/DTR mice. **A:** Emr-1 mRNA expression during skin repair in PBS- and DTox-injected mice as indicated (**left panel**). A quantification of Emr-1 mRNA of the respective RNase protection assay gel is shown in the **right panel**. LysM mRNA expression in 1 day (**B**), 3 day (**C**), 5 day (**D**), 7 day (**E**), and 13 day (**F**) wound tissue in PBS- and DTox-injected mice. Ind 1–4 represent individual *LysM*-Cre/DTR animals as assessed by RNase protection assay (**left panels**). Wt represents a non-transgenic littermate. Every experimental time point depicts three wounds ($n = 3$) isolated from a single individual mouse. Quantifications of lysM mRNA from the respective RNase protection assay gels from day 3, 5, 7, and 13 post-wounding are shown in the **right panels**. $^*P < 0.05$ (unpaired Student's *t*-test) versus PBS-injected mice. Bars indicate the mean ± SD from 15 wounds ($n = 15$) from five individual animals ($n = 5$).

Emr-1 mRNA (macrophage marker) in the presence of elevated lipocalin mRNA (neutrophil marker) expression (Figure 4B). In addition, the neutrophil-specific Gr-1 (Ly-6G) protein was restrictively present only in 7 day wounds of DTox-treated animals (Figure 4C). In accordance to the reduction of macrophages from wounds of DTox-treated *lysM*-Cre/DTR mice (Figure 3A, 4B), we also found a DTox-driven specific loss of macrophages (CD11b high and Ly6C low) during a thioglycollate-induced peritonitis in the animals (Figure 4, D and E). The reduced sensitivity of neutrophils to DTox-mediated cell death might, at least partially, result from a reduced *lysozyme M* promoter activity in the cells. Analysis of adherent, differentiated primary macrophages ($CD11b^+$ and F4/80 high) and freshly isolated neutrophils (Ly6G high) revealed markedly reduced lysozyme M transcript levels in neutrophils (Figure 4F).

Consistent with macrophage-associated Emr-1 (Figure 3A, 4B) and lysM (Figure 3, D and E, and 4B) mRNA signals, wounds of PBS-treated mice were populated by large numbers of wound macrophages (Figure 5A, left panels), whereas overall macrophage numbers appeared markedly reduced in wound tissues on DTox administration of animals (Figure 5A, right panels). Only few macrophages in 7 day wounds from control mice expressed the apoptotic marker active caspase-3, but all remaining wound macrophages in DTox-treated mice appeared in an apoptotic state (Figure 5A, lower panels). In explanation of the elevated lysM mRNA levels in DTox-animals (Figure 3, D and E) in the absence of macrophages (Figure 5A), we found wounds of DTox-administered mice to be extensively infiltrated by neutrophils (Figure 5B). In particular, day 7 wounds exhibit a marked difference with immense numbers of neutrophils throughout the complete wound area on DTox treatment. This condition was strongly contrasted by neutrophil-free wounds in control animals (see also Figure 4C). This finding was important to this study: as expected, neutrophils appeared to have an active transcription from *lysM* allele but DTox did not comprehensively deplete neutrophils for reasons that are discussed below.

Impaired Wounds in DTox-Treated Mice Exhibit a Severely Disturbed Expressional Presence of Pro- and Anti-Inflammatory Mediators and Cox-2

We next investigated wound tissue changes that had been caused by ablation of macrophages. Here we show that expression patterns of the prototypical neutrophil- (MIP-2) and macrophage- (MCP-1) attracting chemokines were markedly changed. MIP-2 mRNA (Figure 6, A and B) and protein (Figure 6C) levels remained elevated in wounds from DTox-treated mice. Remarkably, the prolonged expression of MIP-2 appeared to be, at least partially, a consequence of a prolonged expression of the protein from wound margin keratinocytes (Figure 6D, right panels). In addition, MCP-1 mRNA (Figure 7, A and B) and protein (Figure 7C) expression also appeared elevated in wounds on macrophage ablation. In accordance to both chemokines, we also found the inflammatory cytokine IL-1β to be markedly elevated at the mRNA and protein level as a result of DTox-mediated wound macrophage-depletion (Figure 8, A and B). By contrast, mRNA of the potent anti-inflammatory mediator TGFβ1 appeared reduced in particular at late stages of repair (Figure 8C).

Here we assessed a possible mechanism in the control of the observed prolonged chemokine biosynthesis, possibly from the wound epithelium. As shown in Figure 9A, TGF-β1 mediated a marked reduction in MIP-2 protein release from cytokine-stimulated murine primary keratinocytes. To assess the potency of *ex vivo* wound lysates from *lysM*-Cre/DTR mice to directly stimulate keratinocyte chemokine production *in vitro*, we used the human keratinocyte cell line HaCaT[20] which is responsive to TGF-β1.[18] Human HaCaT cells allow a distinct discrimination between *in vitro*-induced IL-8 (which represents the human

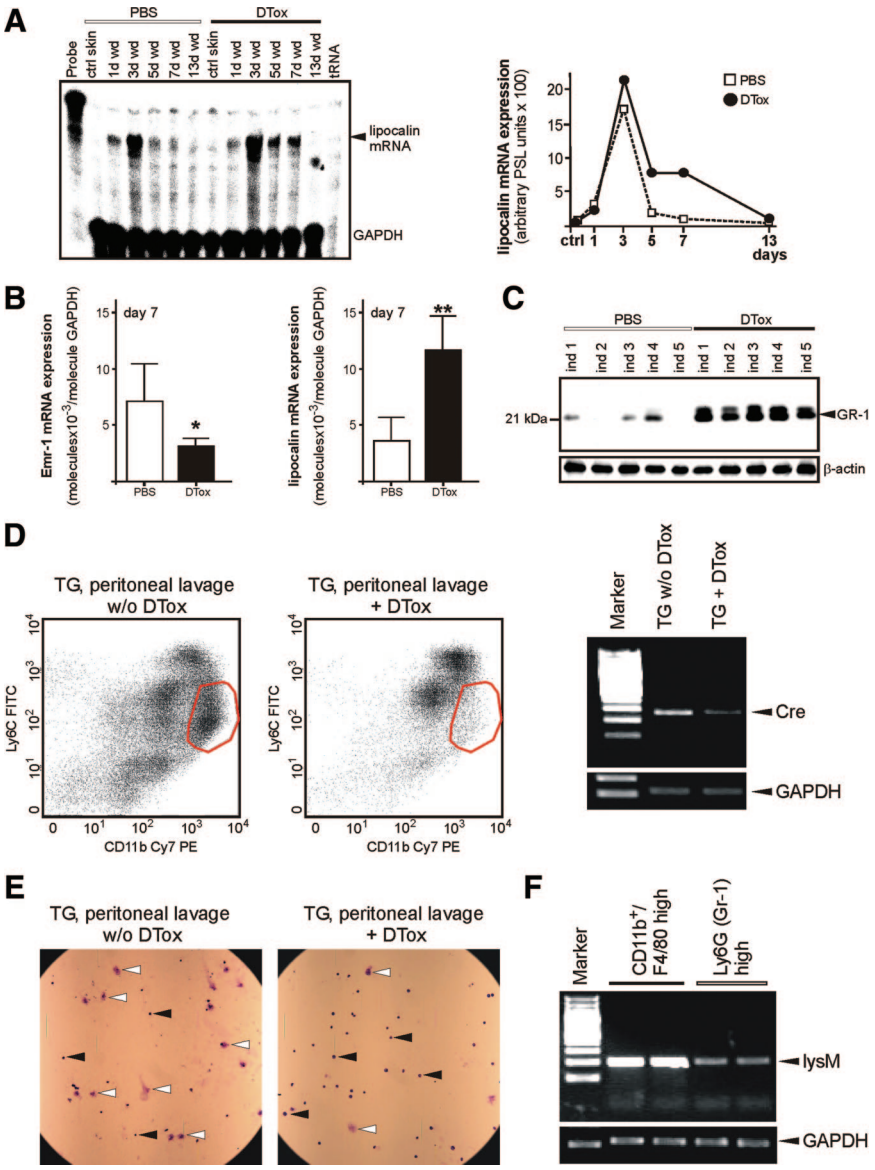

Figure 4. Analysis of wound neutrophils in DTox-injected *lysM*-Cre/DTR mice. **A:** LysM mRNA expression during skin repair in PBS- and DTox-injected mice as indicated (**left panel**). A quantification of lysM mRNA from data points of the respective RNase protection assay gel is shown in the **right panel**. **B:** qRT-PCR quantifications of Emr-1 (**left panel**) and lipocalin (**right panel**) mRNA expression from 7 day wound tissue from five individual mice ($n = 5$) to demonstrate the individual variability of the respective signal. Bars indicate the mean ± SD obtained from wounds ($n = 3$) isolated from five individual animals ($n = 5$). $^{**}P < 0.01$; $^{*}P < 0.05$ (unpaired Student's *t*-test) as compared with PBS-treated mice. **C:** 50 μg of total protein from 7 day wounds of PBS- and DTox-injected mice was analyzed by immunoblot for the presence of the neutrophil surface marker protein GR-1. Every single data point depicts 2 wounds ($n = 2$) from a single individual animal (ind 1–5). β-actin was used to control equal loading. **D:** Peritoneal cellular isolates from a thioglycollate (TG)-induced peritonitis in *lysM*-Cre/DTR after 5 days. 24 hours before isolation of cells from the peritoneum, mice were injected with DTox (TG + DTox) or PBS (TG w/o DTox). Isolated cell fractions were analyzed by FACS. The **red circle** determines the macrophage fraction (CD11b high, Ly6C low). RT-PCR analysis showing Cre mRNA expression in the respective peritoneal cellular isolates from TG-treated mice in the presence (TG + DTox) or absence (TG w/o DTox) of DTox. Pooled isolates from 3 mice are shown on each lane. An amplification of GAPDH is shown for equal loading. **E:** Microscopic view on isolated peritoneal cellular isolates from TG-treated mice in the presence (TG + DTox) or absence (TG w/o DTox) of DTox. **White arrows**, macrophages; **black arrows**, neutrophils or monocytes. **F:** RT-PCR analysis showing lysM mRNA expression in bone marrow-derived, *in vitro*-differentiated macrophages ($CD11b^+$/F4/80 high) and freshly isolated neutrophils (Ly6G high) as indicated. 2 independent preparations are shown for each cell fraction. An amplification of GAPDH is shown for equal loading.

functional homologue of rodent MIP-2) and wound-derived MIP-2, which was present in mouse wound lysates (Figure 6C) used for subsequent HaCaT keratinocyte stimulation. Interestingly, pre-incubation of freshly prepared 5-day wound lysates from both PBS- and DTox-treated *lysM*-Cre/DTR mice with a pan-specific TGF-β1–3 neutralizing antibody did not result in a reduction of induced IL-8 biosynthesis from keratinocytes (Figure 9B). Wound-derived TGF-β bioactivity and neutralizing capability of the antibody were controlled using an *in vitro* assay based on mink lung epithelial cells containing a truncated TGF-β sensitive *plasminogen activator inhibitor-1* promoter fused to the firefly *luciferase* reporter gene.[21] In accordance to data on IL-8 release, wound lysates from PBS- and DTox-treated mice did not differ in bioavailable TGF-β (Figure 9C). By contrast, inhibition of IL-1 receptor signaling significantly reduced IL-8 release from HaCaT keratinocytes on treatment with 5-day wound lysates from macrophage-depleted mice (Figure 9D).

The pro-inflammatory enzyme Cox-2[31] was chosen as marker for inflammatory processes in skin repair.[32] Indeed, also the Cox-2 enzyme was markedly dysregulated, at both the mRNA (Figure 10, A and B) and protein (Figure 10C) level. Notably, Cox-2 protein, elevated in particular during late acute repair (day 7), was mainly expressed in wound margin keratinocytes (Figure 10D), which appeared to be the main cellular source of the enzyme in DTox-treated mice despite its localization in remaining wound macrophages in control mice (Figure 10D, left panels).

DTox-Mediated Depletion of Wound Macrophages Alters Temporal and Spatial Expression Patterns of VEGF

Resident wound margin keratinocytes and infiltrating macrophages express VEGF at the wound site.[33] Nota-

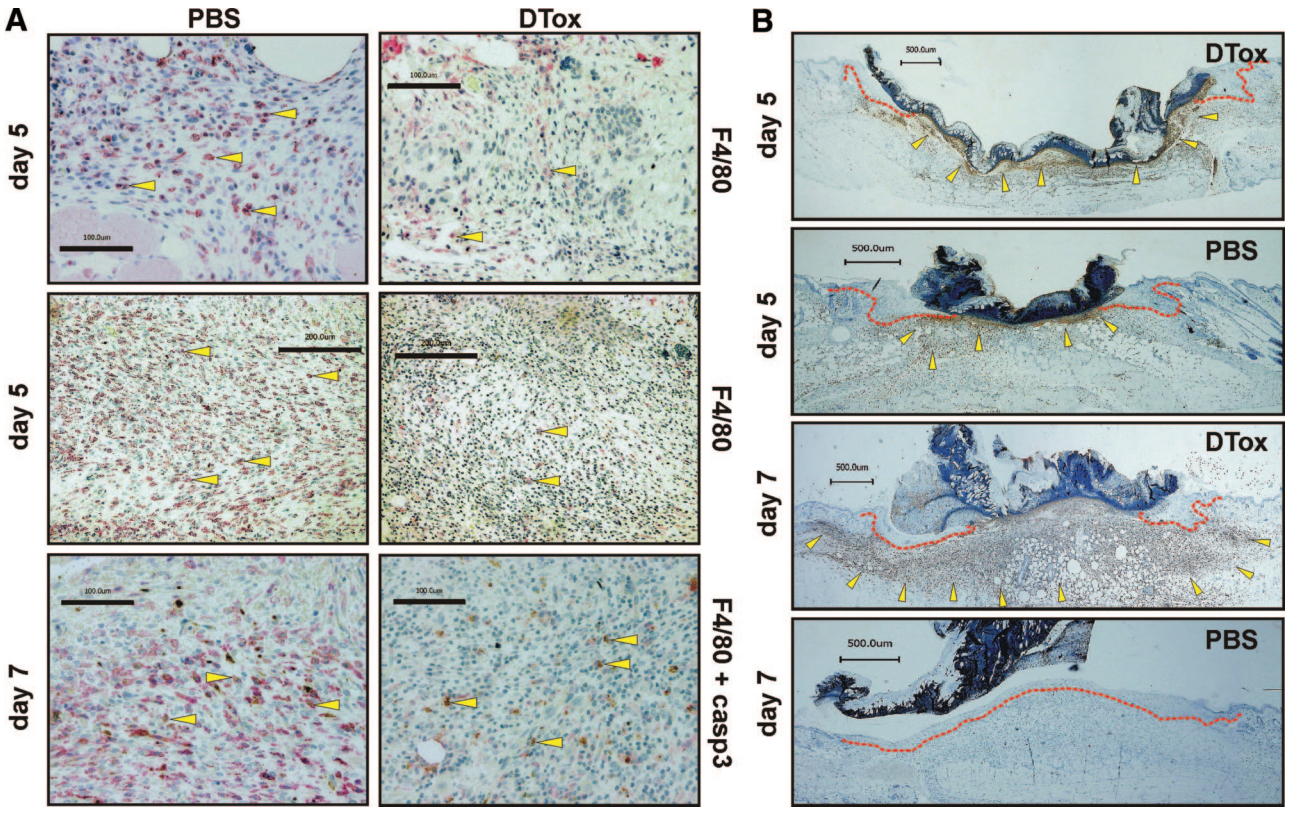

Figure 5. DTox eliminates macrophages from wound tissue. Paraffin sections from day 5 and 7 wounds isolated from PBS- and DTox-injected mice as indicated were incubated with antibodies directed against macrophage-specific F4/80 and active caspase-3 (**A**) or neutrophil-specific GR-1 (**B**) protein. Immunopositive signals were indicated by **yellow arrows**. The epithelial wound margins are indicated by a **red line** in (**B**). Scale bars are given in the photographs.

bly, we could not observe significant changes in wound VEGF mRNA levels on DTox-treatment (Figure 11, A and B), but in the spatial and temporal pattern of wound VEGF protein expression. As shown in Figure 11C, appropriately healing 5-day wounds from PBS-treated mice showed significantly higher levels of $VEGF_{165}$ protein, whereas disturbed wounds from a later phase of repair (day 7) now exhibited increased $VEGF_{165}$ levels (Figure 10D). These expressional changes could be explained by a temporal shift of VEGF expression in wound margin keratinocytes. Proliferating wound margin keratinocytes represented one major source of VEGF in non-disturbed 5-day wounds. By contrast, hyperproliferative keratinocytes from macrophage-depleted wounds appeared to only weakly express VEGF protein at that time point (Figure 11D, upper panels), but showed a robust VEGF-specific signal at a later time point of repair (day 7), when VEGF expression had still been shut off in keratinocytes during normal healing (Figure 11D, lower panels). Interestingly, we also observed VEGF expression in neutrophils on macrophage depletion (Figure 11D). The dysregulated spatial and temporal patterns of VEGF expression at wound sites of DTox-treated mice were subsequently associated with a severely impaired neo-vascularization process. Depletion of macrophages resulted in a nearly complete loss of new vessel formation, as CD31-positive endothelial cells fail to organize into a dense neovasculature that could be observed in PBS-treated control animals (Figure 11E).

Ablation of Wound Macrophages Prevents Myofibroblast Differentiation and Appropriate Wound Contraction

Finally, we investigated the appearance of differentiated myofibroblasts at the wound site, as we had observed a DTox-mediated delay in wound contraction (Figure 2). To this end, we assessed the ED-A splice variant of fibronectin as well as α-SMA mRNA and protein expression (Figure 12, A and B), as markers of the final differentiation of myofibroblasts.[34,35] We observed a clear delay in the appearance of transcripts representing the ED-A variant of fibronectin (Figure 12A) and α-SMA (Figure 12B, right panel). Moreover, the dramatic failure of fibroblasts to differentiate into myofibroblasts in the absence of macrophages at the wound site could be shown most impressively at the protein level, where *de novo* appearance of α-SMA protein was not visible earlier than day 13 of repair (Figure 12B, right panel). These data were strongly confirmed by histology, which revealed a nearly complete absence of α-SMA-positive and thus differentiated myofibroblasts in macrophage-depleted wounds (Figure 12C).

Discussion

The macrophage remains in the focus of scientific interest because of its integrative functions in a large diversity

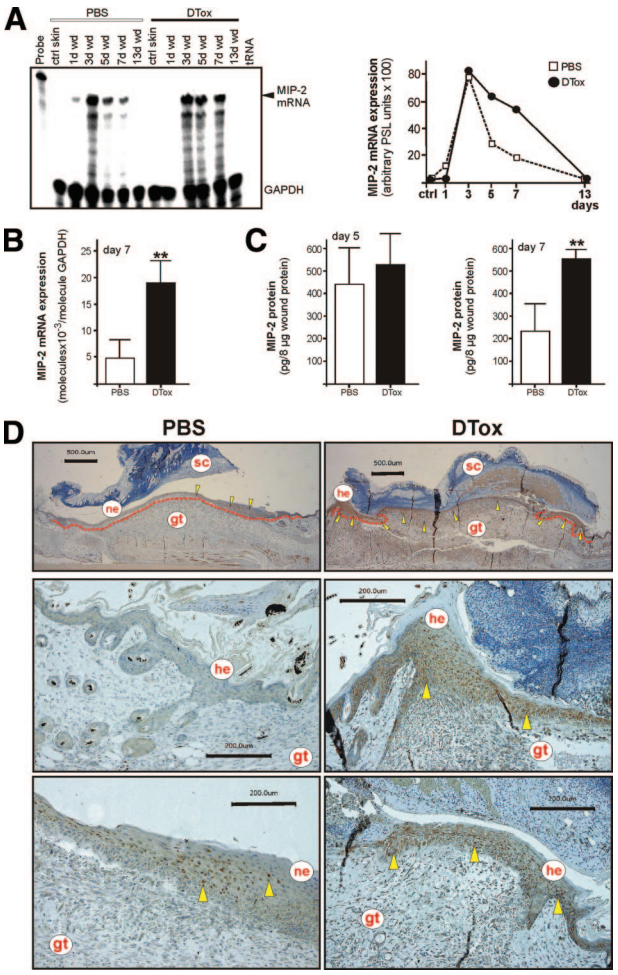

Figure 6. MIP-2 expression in macrophage-depleted wounds. **A:** MIP-2 mRNA expression during skin repair in PBS- and DTox-injected mice as indicated (**left panel**). A quantification of MIP-2 mRNA from data points of the respective RNase protection assay gel is shown in the **right panel**. **B:** qRT-PCR quantifications of MIP-2 mRNA expression from 7 day wound tissue from five individual mice ($n = 5$) to demonstrate the individual variability of the respective signal. Bars indicate the mean ± SD obtained from wounds ($n = 3$) isolated from five individual animals ($n = 5$). $^{**}P < 0.01$ (unpaired Student's *t*-test) as compared with PBS-treated mice. **C:** MIP-2 specific ELISA analyses from 5 day (**left panel**) and 7 day (**right panel**) wound lysates from PBS- and DTox-injected mice. MIP-2 protein is expressed as pg/8 µg skin or section lysate. Bars indicate the mean ± SD obtained from wounds ($n = 2$) isolated from five animals ($n = 5$). $^{**}P < 0.01$ (unpaired Student's *t*-test) as compared with PBS-treated mice. **D:** Paraffin sections from day 7 wound tissue isolated from PBS- and DTox-injected mice were incubated with an antibody directed against MIP-2 protein. Immunopositive signals were indicated by **yellow arrows**. The epithelial wound margins are indicated by a **red line** in the **upper panels**. Scale bars are given in the photographs. gt, granulation tissue; he, hyperproliferative epithelium; ne, neo-epithelium; sc, scab.

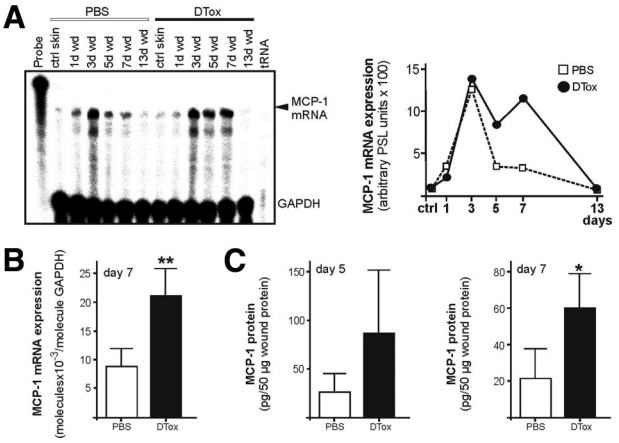

Figure 7. MCP-1 expression in macrophage-depleted wounds. **A:** MCP-1 mRNA expression during skin repair in PBS- and DTox-injected mice as indicated (**left panel**). A quantification of MIP-2 mRNA from data points of the respective RNase protection assay gel is shown in the **right panel**. **B:** qRT-PCR quantifications of MCP-1 mRNA expression from 7-day wound tissue from five individual mice ($n = 5$) to demonstrate the individual variability of the respective signal. Bars indicate the mean ± SD obtained from wounds ($n = 3$) isolated from five individual animals ($n = 5$). $^{**}P < 0.01$ (unpaired Student's *t*-test) as compared with PBS-treated mice. **C:** MCP-1 specific ELISA analyses from 5 day (**left panel**) and 7 day (**right panel**) wound lysates from PBS- and DTox-injected mice. MCP-1 protein is expressed as pg/50 µg skin or section lysate. Bars indicate the mean ± SD obtained from wounds ($n = 2$) isolated from five animals ($n = 5$). $^{*}P < 0.05$ (unpaired Student's *t*-test) as compared with PBS-treated mice.

of physiological and pathophysiological processes, including tissue regeneration. Macrophage numbers are elevated in human chronic leg ulcers[36,37] and wounds in genetically diabetic and obese *db/db* and *ob/ob* mouse models.[28,29] Depletion of wound macrophages by an antibody-based strategy rapidly dampened the excessive inflammation and restored the disturbed tissue regeneration in these animals.[38,39] Macrophage depletion from disturbed wound sites of diabetic mice suggested that the established prime role of this inflammatory cell type might be revised, or at least questioned. 'Classical' studies by Leibovich and Ross had demonstrated that the depletion of macrophages resulted in the failure to clear wound tissue of matrix, dead and damaged cells, fibrin, and debris.[2] However, more recent wound healing studies in PU.1 null mice again question this prime role of macrophages to drive a successful skin repair.[14] PU.1 is a transcription factor pivotally involved in the maturation of hematopoietic cells; its deficiency in PU.1 null mice led to mice without macrophages and functional neutrophils.[40] Wounding of these mice revealed a macrophage-less, scar-free healing that was associated with an absence of an inflammatory response at the wound site.[14] Also prenatal wounds in embryos heal without inflammation and scarring as long as the macrophage lineage has not been developed.[13] Although the studies in PU.1 null mice and embryos added a novel view on the role of macrophages in tissue repair, both experimental setups occurred under sterile conditions.

In the present study, we established the *lysM*-Cre/DTR mouse, which is characterized by a restricted expression of a functional diphtheria toxin receptor in the myeloid cell lineage of double transgenic animals. The myeloid cell-specific expression of the functional DTR is mediated by expression of the Cre recombinase under control of the *lysM* promoter, which is a long-established promoter to drive conditional expression of genes in macrophages and neutrophils.[16,26] *LysM*-driven Cre recombinase excises a *loxP*-flanked transcriptional STOP cassette in front of the DTR open reading frame, thus allowing expression of a DT-sensitive DTR[15] in the myeloid cell lineage of double transgenic *lysM*-Cre/DTR mice. The functionality of this particular model system was based on the finding that murine cells do not express the DTR and therefore

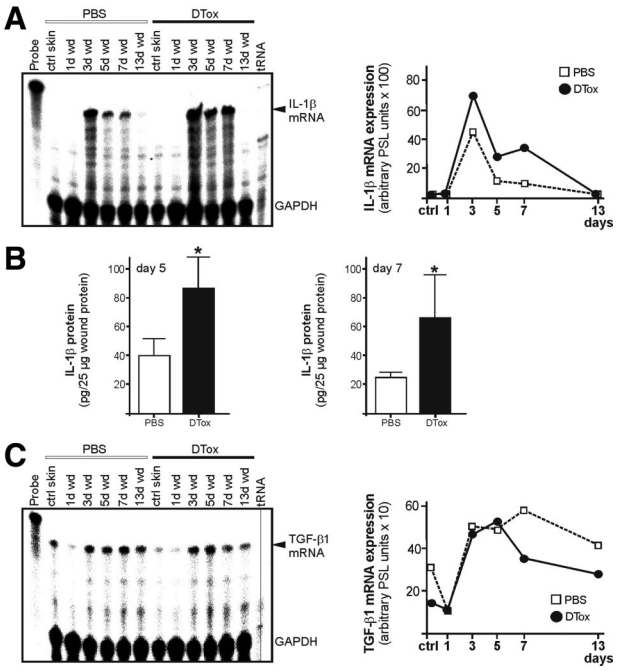

Figure 8. Expression of pro- and anti-inflammatory mediators in macrophage-depleted wounds. **A:** IL-1β mRNA expression during skin repair in PBS- and DTox-injected mice as indicated (**left panel**). A quantification of IL-1β mRNA from data points of the respective RNase protection assay gel is shown in the **right panel**. **B:** IL-1β specific ELISA analyses from 5 day (**left panel**) and 7 day (**right panel**) wound lysates from PBS- and DTox-injected mice. IL-1β protein is expressed as pg/25 μg skin or section lysate. Bars indicate the mean ± SD obtained wounds (n = 2) isolated from five animals (n = 5). $^*P < 0.05$ (unpaired Student's t-test) as compared with PBS-treated mice. **C:** TGF-β1 mRNA expression during skin repair in PBS- and DTox-injected mice as indicated (**left panel**). A quantification of TGF-β1 mRNA from data points of the respective RNase protection assay gel is shown in the **right panel**.

are naturally DTox resistant.[23] This is important for two reasons: conditional expression of the simian HB-EGF in mice will render the respective cells sensitive to DTox[24] and transgenic animals exhibit a normal phenotype, as long as they are not administered with the toxin, a fact that provides the basis of the inducibility of cell ablation.[15] The functionality of this DTR-based inducible model of cell ablation has been shown for myeloid cells: *CD11b*-driven DTR expression was used to efficiently deplete macrophages from liver tissue in a model of liver injury and regeneration.[41]

In this study, we could indeed prove the functionality of this inducible DTox-mediated system to systemically deplete macrophages from transgenic animals and their wounds. Availability of the DTR was dependent of the *lysM* promoter, which targets both macrophages and neutrophils.[16,26] As we had chosen only those transgenic mice for the experiments, which still had one functional allele of the wild-type *lysM* locus, we were able to assess the endogenous lysM mRNA as a marker to document a potential DTox-mediated loss of lysM-expressing cells from wounds. Here it is important to state that our immunohistologic data showed that we indeed could deplete macrophages from wound tissue. For this reason, the remaining robust lysM mRNA signals in acute wound tissue must be conjoined to the immense numbers of neutrophils, which populated wounds of DTox-treated

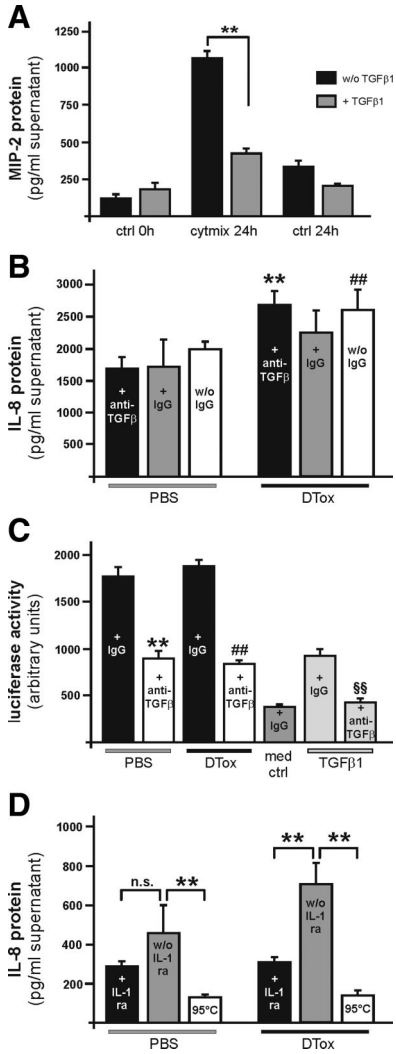

Figure 9. IL-1 signaling pathways contribute to augmented inflammation in macrophage-depleted wounds. **A:** Confluent primary keratinocytes from C57Bl/6J mice were analyzed for the release of MIP-2 in the presence or absence of cytokines (40 ng/ml IL-1β, 25 ng/ml tumor necrosis factor-α, 20 ng/ml U/ml interferon-γ) or TGF-β1 (5 ng/ml) after 20 hours as indicated. $^{**}P < 0.01$ as indicated by the brackets. Bars depict means ± SD obtained from three independent cell culture experiments (n = 3). **B:** Confluent human HaCaT keratinocytes were stimulated with pooled wound lysates (n = 25 wounds from 5 individual animals) (f.c. 100 μg/ml) of PBS- or-DTox-treated *lysM*-Cre/DTR mice. Lysates were treated with an anti-TGFβ antibody (10 μg/ml), a non-specific IgG (10 μg/ml) or left untreated (w/o IgG). IL-8 was determined from cell culture supernatants after 24 by ELISA. **, $^{\#\#}$, $P < 0.01$ as compared with the respective bar in PBS-control. Bars depict means ± SD obtained from three independent cell culture experiments (n = 3). **C:** Mink lung epithelial reporter cells were stimulated with fresh wound lysates (n = 25 wounds from 5 individual animals) (f.c. 400 μg/ml) of PBS- or- DTox-treated lysM-Cre/DTR mice in the presence or absence of an anti-TGFβ antibody (100 μg/ml). Medium containing non-specific IgG (med + IgG), or TGF-β1 (0.8 ng/ml) with non-specific IgG or an anti-TGFβ antibody (100 μg/ml) were used to control reactivity of the reporter cells. TGF-β bioactivity is expressed as stimulation of relative luminescence units (RLU) derived from luciferase enzymatic activity induced from a TGF-β-sensitive plasminogen activator inhibitor promoter in the cells. **D:** Confluent human HaCaT keratinocytes were stimulated with pooled wound lysates (n = 25 wounds from 5 individual animals) (f.c. 100 μg/ml) of PBS- or- DTox-treated *lysM*-Cre/DTR mice. Cells were pre-treated with IL-1ra (500 μg/ml) (+IL-1ra) or left untreated (w/o IL-1ra). Heated lysate (95°C) was used as a control. IL-8 was determined from cell culture supernatants after 24 by ELISA. $^{**}P < 0.01$; n.s, not significant as indicated by the brackets. Bars depict means ± SD obtained from three independent cell culture experiments (n = 3).

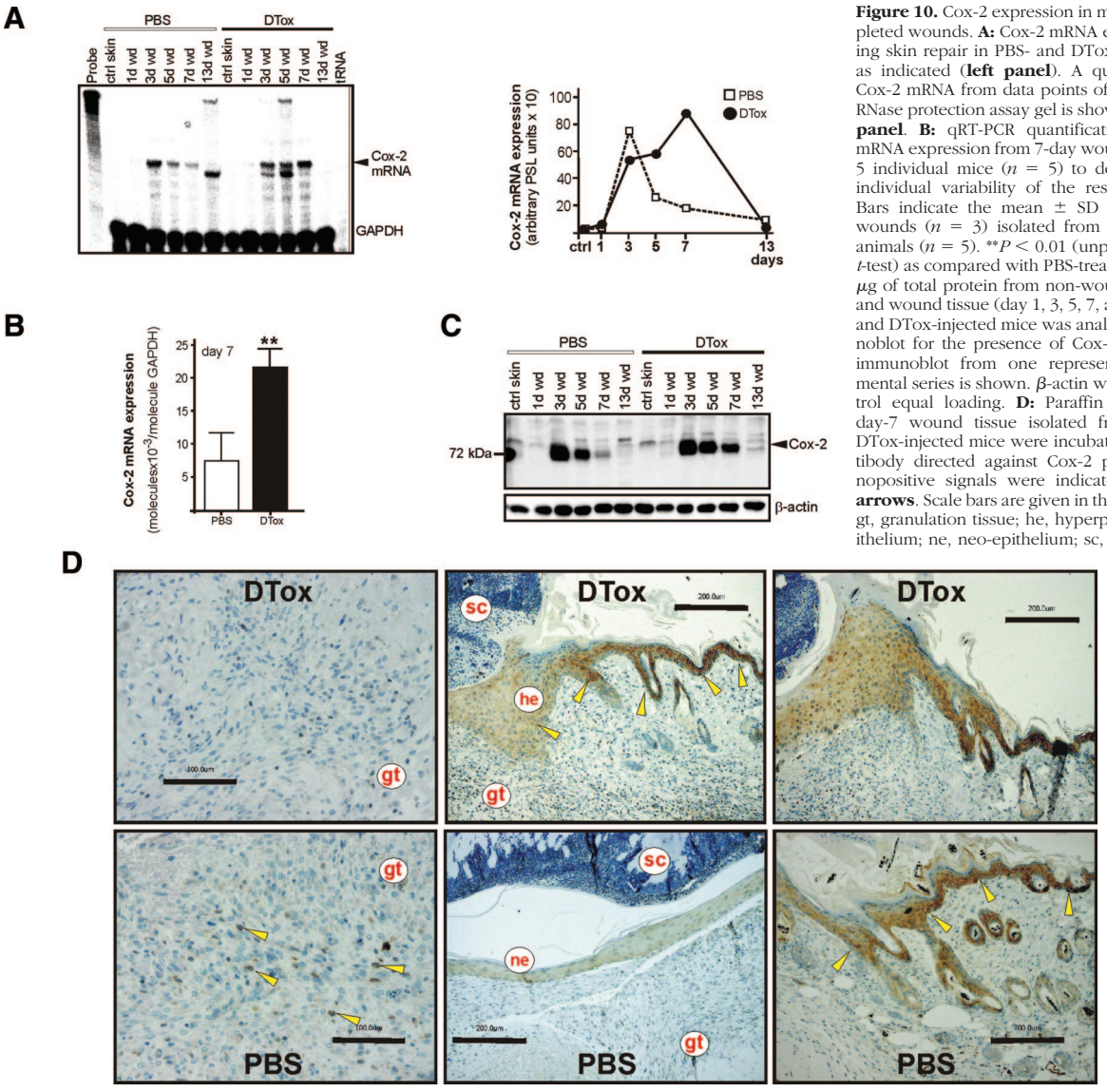

Figure 10. Cox-2 expression in macrophage-depleted wounds. **A:** Cox-2 mRNA expression during skin repair in PBS- and DTox-injected mice as indicated (**left panel**). A quantification of Cox-2 mRNA from data points of the respective RNase protection assay gel is shown in the **right panel**. **B:** qRT-PCR quantifications of Cox-2 mRNA expression from 7-day wound tissue from 5 individual mice ($n = 5$) to demonstrate the individual variability of the respective signal. Bars indicate the mean ± SD obtained from wounds ($n = 3$) isolated from five individual animals ($n = 5$). $^{**}P < 0.01$ (unpaired Student's *t*-test) as compared with PBS-treated mice. **C:** 50 μg of total protein from non-wounded *ctrl* skin and wound tissue (day 1, 3, 5, 7, and 13) of PBS- and DTox-injected mice was analyzed by immunoblot for the presence of Cox-2 protein. The immunoblot from one representative experimental series is shown. β-actin was used to control equal loading. **D:** Paraffin sections from day-7 wound tissue isolated from PBS- and DTox-injected mice were incubated with an antibody directed against Cox-2 protein. Immunopositive signals were indicated by **yellow arrows**. Scale bars are given in the photographs. gt, granulation tissue; he, hyperproliferative epithelium; ne, neo-epithelium; sc, scab.

mice in the absence of macrophages. This finding shows that, despite the potential expression of a functional DTR, DTox appeared not as functional in depleting neutrophils as it was for macrophages. This argument is strengthened by the finding that DTox also specifically depleted a CD11b high and Ly6C low immune cell population from thioglycollate-induced peritoneal infiltrate in *lysM*-Cre/DTR mice. This notion might be functionally linked to a lower activity of the *lysM* promoter in neutrophils as shown in this study (a phenomenon which also likely contributed to the depletion of tissue macrophages but not circulating monocytes from the animals). Moreover, neutrophils possess a short-lived turnover and represent more than 50% of the circulating leukocytes, so that DTox might also fail to efficiently interfere with the huge numbers of neutrophils that infiltrated the wound tissue.

Interestingly, induction of macrophage depletion from skin wounds finally supported the above mentioned findings from Leibovich and Ross.[2] In general, by analyzing prototypical markers in documentation of diverse but pivotal cellular actions in skin repair, we found an exacerbated inflammatory response with increased expression of MIP-2, MCP-1, and Cox-2 in wound tissues, more IL-1β in the presence of reduced TGF-β1 expression, a dysregulated pattern of VEGF and, most importantly, a nearly complete loss of wound contraction in the absence of myofibroblast differentiation. These observations support recent studies in transgenic mice, where reduced numbers of macrophages in wounds of MIP-2- or CXCR2-deficient mice also resulted in a disturbed healing.[3,4]

It is tempting to argue that dense populations of wound neutrophils might influence the production of inflammatory mediators by the wound epithelium. Wound macrophages represent a major cellular source of TGF-β1,[7,9,10] a cytokine with prominent anti-inflammatory actions in mice.[42] However, under conditions of reduced wound tissue macrophages, our data suggest that TGF-β1 might not be of importance in the control of inflammatory re-

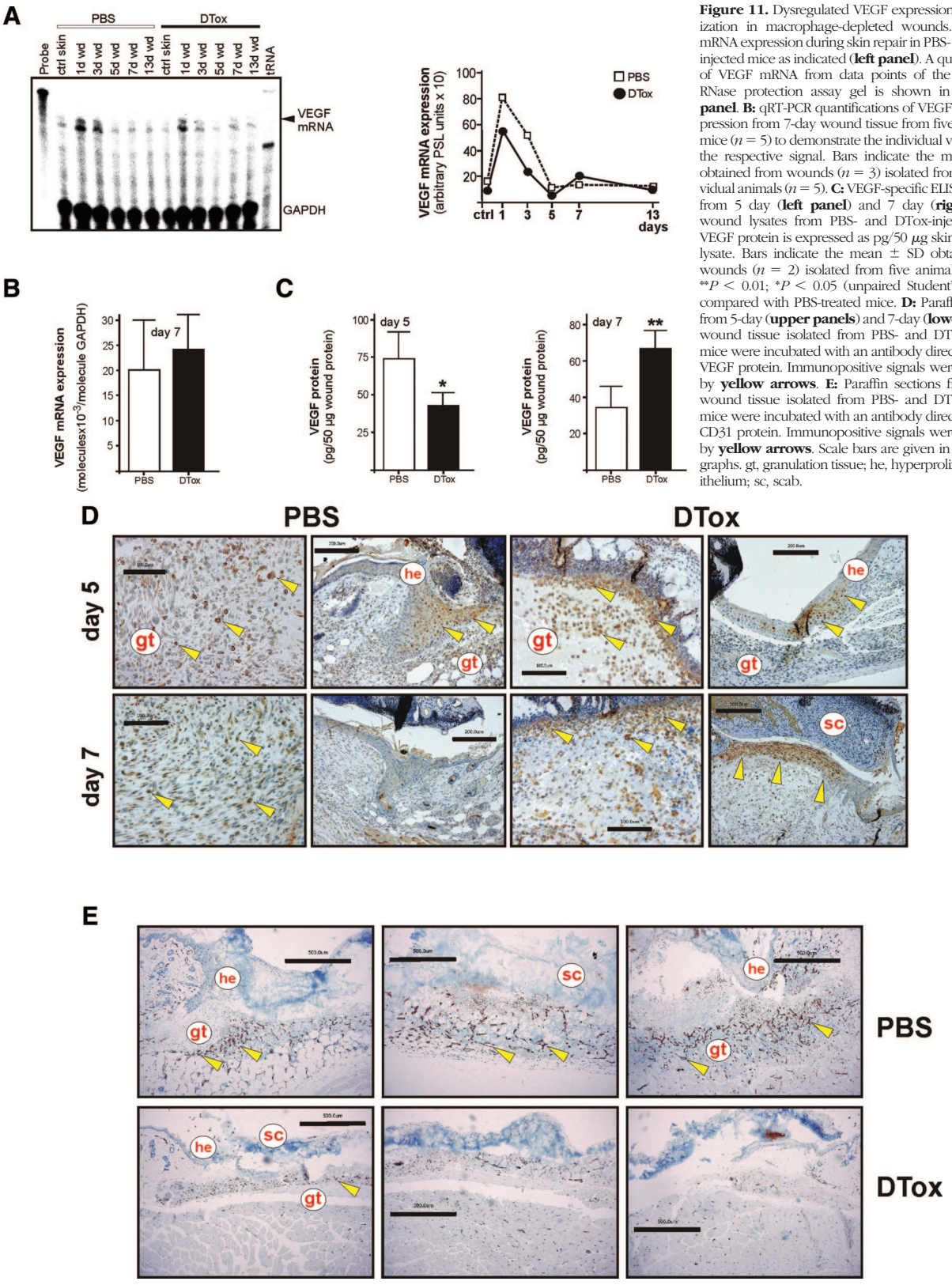

Figure 11. Dysregulated VEGF expression and localization in macrophage-depleted wounds. **A:** VEGF mRNA expression during skin repair in PBS- and DTox-injected mice as indicated (**left panel**). A quantification of VEGF mRNA from data points of the respective RNase protection assay gel is shown in the **right panel**. **B:** qRT-PCR quantifications of VEGF mRNA expression from 7-day wound tissue from five individual mice ($n = 5$) to demonstrate the individual variability of the respective signal. Bars indicate the mean ± SD obtained from wounds ($n = 3$) isolated from five individual animals ($n = 5$). **C:** VEGF-specific ELISA analyses from 5 day (**left panel**) and 7 day (**right panel**) wound lysates from PBS- and DTox-injected mice. VEGF protein is expressed as pg/50 μg skin or section lysate. Bars indicate the mean ± SD obtained from wounds ($n = 2$) isolated from five animals ($n = 5$). $^{**}P < 0.01$; $^{*}P < 0.05$ (unpaired Student's *t*-test) as compared with PBS-treated mice. **D:** Paraffin sections from 5-day (**upper panels**) and 7-day (**lower panels**) wound tissue isolated from PBS- and DTox-injected mice were incubated with an antibody directed against VEGF protein. Immunopositive signals were indicated by **yellow arrows**. **E:** Paraffin sections from day 5 wound tissue isolated from PBS- and DTox-injected mice were incubated with an antibody directed against CD31 protein. Immunopositive signals were indicated by **yellow arrows**. Scale bars are given in the photographs. gt, granulation tissue; he, hyperproliferative epithelium; sc, scab.

sponses of wound keratinocytes, as wound lysates of DTox- and PBS-treated *lysM*-Cre/DTR mice did not differ in bioavailable TGF-β. By contrast, neutrophils are well-known producers of pro-inflammatory cytokines such as IL-1β,[10,43,44] a cytokine that was indeed increased in macrophage-depleted and neutrophil-infiltrated wounds (this study). Neutralization of IL-1 bioactivity from macrophage-depleted wound homogenates reduced the po-

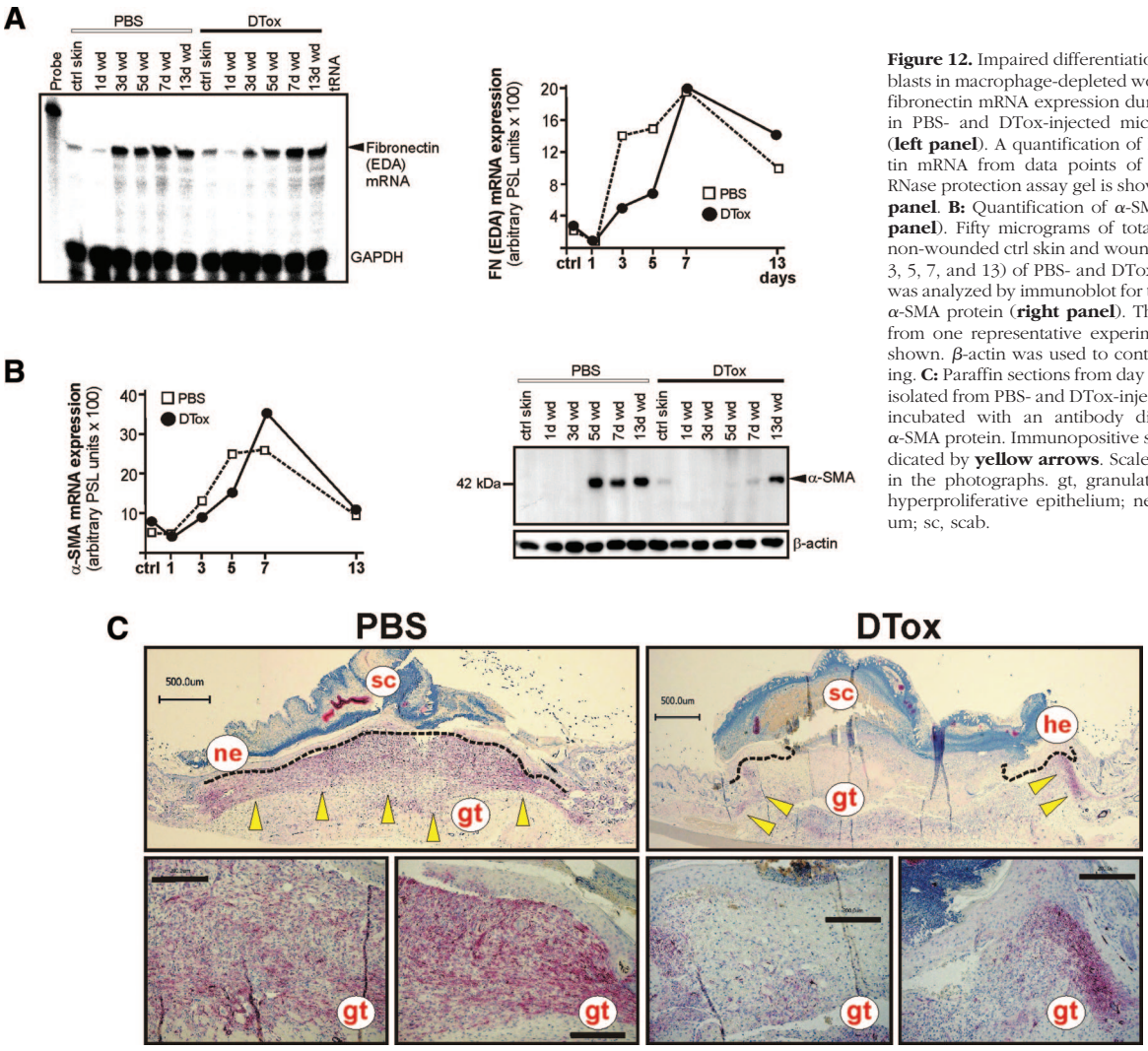

Figure 12. Impaired differentiation of myofibroblasts in macrophage-depleted wounds. **A:** ED-A fibronectin mRNA expression during skin repair in PBS- and DTox-injected mice as indicated (**left panel**). A quantification of ED-A fibronectin mRNA from data points of the respective RNase protection assay gel is shown in the **right panel**. **B:** Quantification of α-SMA mRNA (**left panel**). Fifty micrograms of total protein from non-wounded ctrl skin and wound tissue (day 1, 3, 5, 7, and 13) of PBS- and DTox-injected mice was analyzed by immunoblot for the presence of α-SMA protein (**right panel**). The immunoblot from one representative experimental series is shown. β-actin was used to control equal loading. **C:** Paraffin sections from day 7 wound tissue isolated from PBS- and DTox-injected mice were incubated with an antibody directed against α-SMA protein. Immunopositive signals were indicated by **yellow arrows**. Scale bars are given in the photographs. gt, granulation tissue; he, hyperproliferative epithelium; ne, neo-epithelium; sc, scab.

tency of homogenates to stimulate keratinocyte chemokine production to levels found in control mice. These findings suggest that wound macrophages might control wound neutrophils. At least a partial loss of this control on macrophage-depletion probably changes the inflammatory balance in wounds toward pro-inflammatory responses with an overshooting action of infiltrating neutrophils as a consequence.

In addition, our data confirm the described important functional connection between macrophage and myofibroblast differentiation. It has been shown that myofibroblast differentiation and thus wound contraction was pivotally dependent on macrophage-derived TGF-β1.[5] TGF-β1 is known as the major pathway for transcriptional induction of α-SMA via Smad signaling in differentiating myofibroblasts.[35] Thus, unaltered levels of bioactive TGF-β1 on macrophage-ablation might provide a possible explanation for the nearly unchanged wound α-SMA mRNA levels. Despite the early presence of TGF-β1 in wounds, however, expression of α-SMA is restricted to later phases of repair and controlled by mechanical changes in the wound microenvironment.[35] Thus, a loss of mechanical stimuli in macrophage-ablated and impaired wounds might be responsible for a translational loss of α-SMA protein in the presence of persisting mRNA species.

In summary, our data show that macrophages are necessary to drive a normal, although not perfect healing under normal, non-sterile conditions, and that interference with this function dramatically worsens this process. Moreover, our data suggest the *lysM*-Cre/DTR mouse as a suitable animal model of inducible macrophage depletion to further investigate the role of this immune cell type in tissue repair. In particular, transfer of this animal model into an either genetically or diet-induced obese and diabetic phenotype, will provide an efficient experimental tool to question the potentially deleterious role of obesity-activated macrophages in diabetes-impaired skin repair[39] in the near future.

Acknowledgments

We are grateful to Dr. Rifkin for providing the mink lung epithelial cell line.

References

1. Simpson DM, Ross R: The neutrophilic leukocyte in wound repair: a study with antineutrophil serum. J Clin Invest 1972, 51:200–223
2. Leibovich SJ, Ross R: The role of the macrophage in wound repair: a study with hydrocortisone and antimacrophage serum. Am J Pathol 1975, 78:71–100
3. DiPietro LA, Burdick M, Low QE, Kunkel SL, Strieter RM: MIP-1alpha as a critical macrophage chemoattractant in murine wound repair. J Clin Invest 1998, 101:1693–1698
4. Devalaraja RM, Nanney LB, Du J, Qian Q, Yu Y, Devalaraja MN, Richmond A: Delayed wound healing in CXCR2 knockout mice. J Invest Dermatol 2000, 115:234–244
5. Peters T, Sindrilaru A, Hinz B, Hinrichs R, Menke A, Al-Azzeh EA, Holzwarth K, Oreshkova T, Wang H, Kess D, Walzog B, Sulyok S, Sunderkötter C, Friedrich W, Wlaschek M, Krieg T, Scharffetter-Kochanek K: Wound healing defect of CD18−/− mice due to a decrease in TGF-β1 and myofibroblast differentiation. EMBO J 2005, 24:3400–3410
6. Low QE, Drugea IA, Duffner LA, Quinn DG, Cook DN, Rollins BJ, Kovacs EJ, DiPietro L: Wound healing in MIP-1 alpha (−/−) and MCP-1 (−/−) mice. Am J Pathol 2001, 159:457–463
7. Martin P: Wound healing - aiming for perfect skin regeneration. Science 1997, 276:75–81
8. Singer AJ, Clark RAF: Cutaneous wound healing. N Engl J Med 1999, 341:738–746
9. Werner S, Grose R: Regulation of wound healing by growth factors and cytokines. Physiol Rev 2003, 83:835–870
10. Eming SA, Krieg T, Davidson JM: Inflammation in wound repair: molecular and cellular mechanisms. J Invest Dermatol 2007, 127:514–525
11. Ashcroft GS, Yang X, Glick AB, Weinstein M, Letterio JL, Mizel DE, Anzano M, Greenwell-Wild T, Wahl SM, Deng C, Roberts AB: Mice lacking Smad3 show accelerated wound healing an impaired local inflammatory response. Nat Cell Biol 1999, 1:E117–E119
12. Mori R, Kondo T, Ohshima T, Ishida Y, Mukaida N: Accelerated wound healing in tumor necrosis factor receptor p55-deficient mice with reduced leukocyte infiltration. FASEB J 2002, 16: 963–974
13. Hopkinson-Woolley J, Hughes D, Gordon S, Martin P: Macrophage recruitment during limb development and wound healing in the embryonic and foetal mouse. J Cell Sci 1994, 107:1159–1167
14. Martin P, D'Souza D, Martin J, Grose R, Cooper L, Maki R, McKercher SR: Wound healing in the PU. 1 null mouse – tissue repair is not dependent on inflammatory cells. Curr Biol 2003, 13:1122–1128
15. Buch T, Heppner FL, Tertilt C, Heinen TJ, Kremer M, Wunderlich FT, Jung S, Waisman A: A Cre-inducible diphteria toxin receptor mediates cell lineage ablation after toxin administration. Nat Methods 2005, 2:419–426
16. Clausen BE, Burkhardt C, Reith W, Renkawitz R, Förster I: Conditional gene targeting in macrophages and granulocytes using LysMcre mice. Transgenic Res 1999, 8:265–277
17. Stallmeyer B, Kämpfer H, Kolb N, Pfeilschifter J, Frank S: The function of nitric oxide in wound repair: inhibition of inducible nitric oxide synthase severely impairs wound reepithelialization. J Invest Dermatol 1999, 113:1090–1098
18. Frank S, Stallmeyer B, Kämpfer H, Kolb N, Pfeilschifter J: Nitric oxide triggers enhanced induction of vascular endothelial growth factor expression in cultured keratinocytes (HaCaT) and during cutaneous wound repair. FASEB J 1999, 13:2002–2014
19. Chomczynski P, Sacchi N: Single-step method of RNA isolation by acid guanidinium thiocyanate-phenol-chloroform extraction. Anal Biochem 1987, 162:156–159
20. Boukamp P, Petrussevska RT, Breitkreutz D, Hornung J, Markham A, Fusenig NE: Normal keratinization in a spontaneously immortalized aneuploid human keratinocyte cell line. J Cell Biol 1988, 106:761–771
21. Abe M, Harpel JG, Metz CN, Nunes I, Loskutoff DJ, Rifkin DB: An assay for transforming growth factor-beta using cells transfected with a plasminogen activator inhibitor-1 promoter-luciferase construct. Anal Biochem 1994, 216:276–284
22. Naglich JG, Metherall JE, Russell DW, Eidels L: Expression cloning of a diphteria toxin receptor: identity with a heparin-binding EGF-like growth factor precursor. Cell 1992, 69:1051–1061
23. Middlebrook JL, Dorland RB: Response of cultured mammalian cells to the exotoxins of Pseudomonas aeruginosa and Corynebacterium diphteriae: differential cytotoxicity. Can J Microbiol 1977, 23:183–189
24. Saito M, Iwawaki T, Taya C, Yonekawa H, Noda M, Inui Y, Mekada E, Kimata Y, Tsuru A, Kohno K: Diphtheria toxin receptor-mediated conditional and targeted cell ablation in transgenic mice. Nature Biotechnol 2001, 19:746–750
25. Zambrowicz BP, Imamoto A, Fiering S, Herzenberg LA, Kerr WG, Soriano P: Disruption of overlapping transcripts in the ROSA beta geo 26 gene trap strain leads to widespread expression of beta-galactosidase in mouse embryos and hematopoietic cells. Proc Natl Acad Sci USA 1997, 94:3789–3794
26. Faust N, Varas F, Kelly LM, Heck S, Graf T: Insertion of enhanced green fluorescent protein into the lysozyme gene creates mice with green fluorescent granulocytes and macrophages. Blood 2000, 96:719–726
27. Austyn JM, Gordon S: F4/80, monoclonal antibody directed specifically against the mouse macrophage. Eur J Immunol 1981, 11:805–815
28. Wetzler C, Kämpfer H, Stallmeyer B, Pfeilschifter J, Frank S: Large and sustained induction of chemokines during impaired wound healing in the genetically diabetic mouse: prolonged persistence of neutrophils and macrophages during the late phase of repair. J Invest Dermatol 2000, 115:245–253
29. Goren I, Kämpfer H, Podda M, Pfeilschifter J, Frank S: Leptin and wound inflammation in diabetic ob/ob mice: differential regulation of neutrophil and macrophage influx and a potential role for the scab as a sink for inflammatory cells and mediators. Diabetes 2003, 52:2821–2832
30. McKnight AJ, Macfarlane AJ, Dri P, Turley L, Willis AC, Gordon S: Molecular cloning of F4/80, a murine macrophage-restricted cell surface glycoprotein with homology to the G-protein-linked transmembrane 7 hormone receptor family. J Biol Chem 1996, 271:486–489
31. Smith WL, DeWitt DL, Garavito RM: Cyclooxygenases: structural, cellular, and molecular biology. Annu Rev Biochem 2000, 69:145–182
32. Kämpfer H, Schmidt R, Geisslinger G, Pfeilschifter J, Frank S: Wound inflammation in diabetic ob/ob mice: functional coupling of prostaglandin biosynthesis to cyclooxygenase-1 activity in diabetes-impaired wound healing. Diabetes 2005, 54:1543–1551
33. Brown LF, Yeo KT, Berse B, Yeo TK, Senger DR, Dvorak HF, van de Water L: Expression of vascular permeability factor (vascular endothelial growth factor) by epidermal keratinocytes during wound healing. J Exp Med 1992, 176:1375–1379
34. Tomasek JJ, Gabbiani G, Hinz B, Chaponnier C, Brown RA: Myofibroblasts and mechanoregulation of connective tissue remodelling. Nat Rev Cell Biol 2002, 3:349–363
35. Hinz B: Formation and function of the myofibroblast duringt tissue repair. J Invest Dermatol 2007, 127:526–537
36. Rosner K, Ross C, Karlsmark T, Petersen AA, Gottrup F, Vejlsgaard GL: Immunohistochemical characterization of the cutaneous cellular infiltrate in different areas of chronic leg ulcers. APMIS 1995, 103:293–299
37. Loots MA, Lamme EN, Zeegelar J, Mekkes JR, Bos JD, Middelkoop E: Differences in cellular infiltrate and extracellular matrix of chronic diabetic and venous ulcers versus acute wounds. J Invest Dermatol 1998, 111:850–857
38. Goren I, Müller E, Pfeilschifter J, Frank S: Severely impaired insulin signaling in chronic wounds of diabetic ob/ob mice: a potential role of tumor necrosis factor-alpha. Am J Pathol 2006, 168:765–777
39. Goren I, Müller E, Schiefelbein D, Christen U, Pfeilschifter J, Mühl H, Frank S: Systemic anti-TNFalpha treatment restores diabetes-impaired skin repair in ob/ob mice by inactivation of macrophages. J Invest Dermatol 2007, 127:2259–2267
40. McKercher SR, Torbett BE, Anderson KL, Henkel GW, Vestal DJ, Baribault H, Klemsz M, Feeney AJ, Wu GE, Paige CJ, Maki RA: Targeted disruption of the PU. 1 gene results in multiple hematopoietic abnormalities. EMBO J 1996, 15:5647–5658
41. Duffield JS, Forbes SJ, Constandinou CM, Clay S, Partolina M, Vuthoori S, Wu S, Lang R, Iredale JP: Selective depletion of macrophages reveals distinct, opposing roles during liver injury and repair. J Clin Invest 2005, 115:56–65

42. Kulkarni AB, Huh CG, Becker D, Geiser A, Lyght M, Flanders KC, Roberts AB, Sporn MB, Ward JM, Karlsson S: Transforming growth factor β1 null mutation in mice causes excessive inflammatory responses and early death. Proc Natl Acad Sci USA 1993, 90:770–774
43. Hübner G, Brauchle M, Smola H, Madlener M, Fässler R, Werner S: Differential regulation of pro-inflammatory cytokines during wound healing in normal and glucocorticoid-treated mice. Cytokine 1996, 8:548–556
44. Goren I, Kämpfer H, Müller E, Schiefelbein D, Pfeilschifter J, Frank S: Oncostatin M expression is functionally connected to neutrophils in the early inflammatory phase of skin repair: implications for normal and diabetes-impaired wounds. J Invest Dermatol 2006, 126: 628–637